Tuning Forks and Galactic Centers

Francisco Duque
CENTRA, Instituto Superior Tecnico, University of Lisbon

GReCO Webinar, 15th March, 2021

grit gravitation in técnico

centra

FCT Fundação para a Ciência e a Tecnologia

cost EUROPEAN COOPERATION IN SCIENCE & TECHNOLOGY

Outline

1. Why galactic centers?

2. Hierarchical triple systems: a gravitational tuning fork
Cardoso, Duque and Khanna, arXiv:2101.01186 (2021)

3. Accretion of luminous matter: *the* light ring to rule them all
Cardoso, Duque and Foschi, arXiv:2102.07784 (2021)

4. Future directions

The Gravitational Wave Era (2015-)

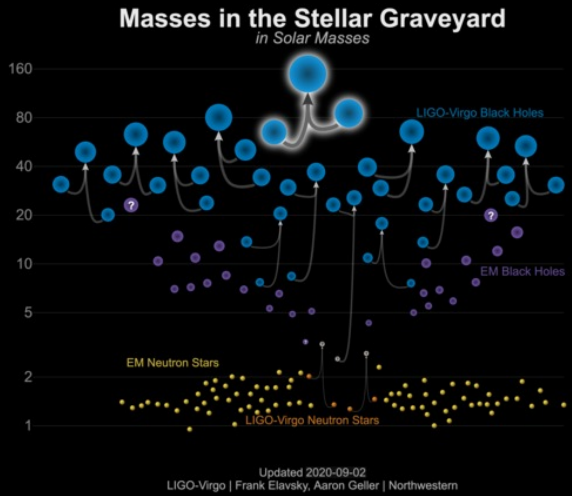

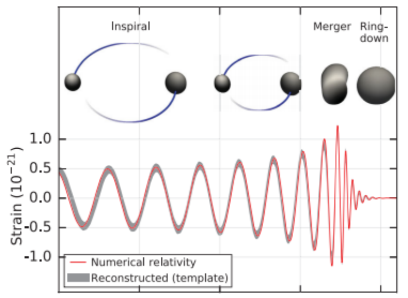

GW150914

LIGO-Virgo Collab., PRL 116.061102 (2016)

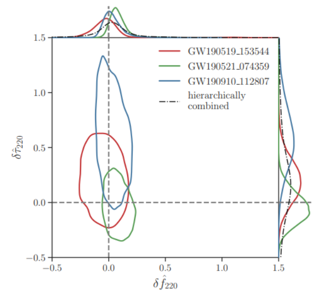

Ringdown tests

LIGO-Virgo Collab., arXiv:2010.14529 (2020)

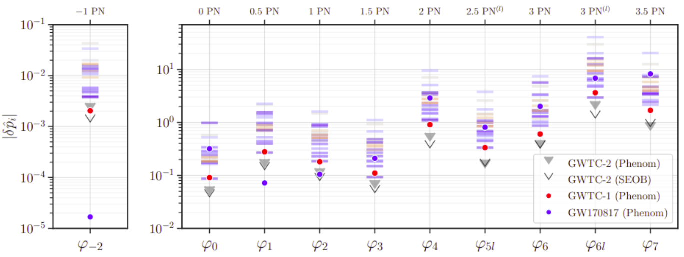

PN deviations of GR

LIGO-Virgo Collab., arXiv:2010.14529 (2020)

KAGRA *(Image Credit: ICRR, Univ. of Tokyo)*

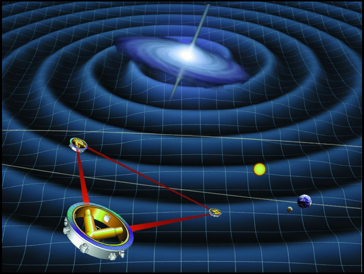

LISA mission *(Image Credit: ESA)*

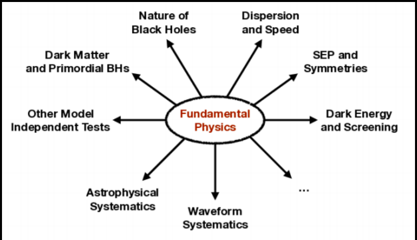

LISA taxonomy
(Image Credit: Barausse et al., Gen.Rel.Grav. 52, 81 (2020))

The Curious Case of GW190521

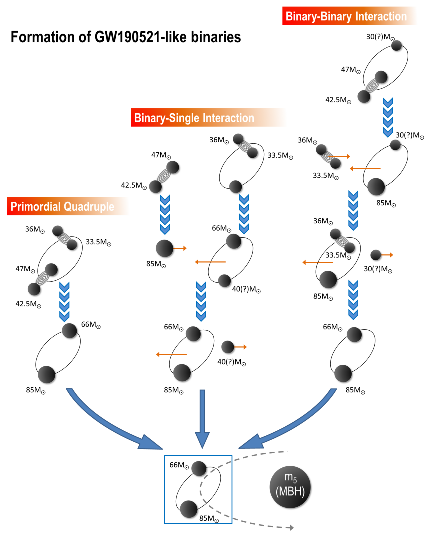

Bin Liu and Dong Lai arXiv:2009.10068

*"We report the first plausible optical electromagnetic counterpart to a (candidate) binary black hole merger. Detected by the Zwicky Transient Facility, the EM flare is consistent with expectations for a kicked **BBH merger in the accretion disk of an active galactic nucleus** (AGN)"*

M. J. Graham et al., PRL 124.251102 (2020)

Merger rate:

$$f_{\mathrm{merger}_{2G}} \sim 0.6 - 6\,\mathrm{Gpc}^{-3}\mathrm{yr}^{-1}$$

LIGO-Virgo Collaboration, ApJL, 892 L3 (2020)

Hierarchical triple systems

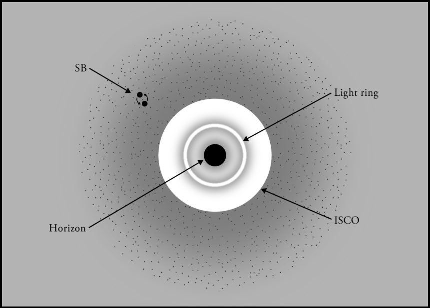

Image Credit: Ana Sousa Carvalho

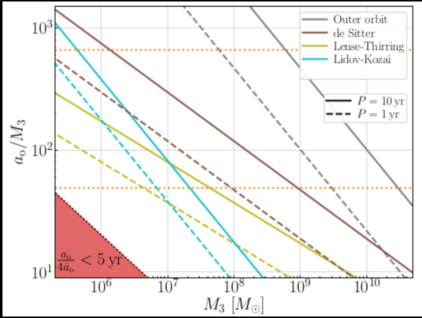

Yu and Chen, PRL 126.021101 (2021)

Conservation of L_z

$$(1 - e_{\rm in}^2)\cos^2\iota = \text{const}$$

If $39^o < \iota < 141^o$

$$\omega_{\rm Pericenter} = \pi \text{ or } 3\pi/2$$

$$t_{\rm KL} \sim P_{\rm in}\frac{m_{\rm in}}{M}\left(\frac{a_{\rm out}}{a_{\rm in}}\right)^3 (1 - e_{\rm out}^2)^{3/2}$$

Kozai-Lidov resonances

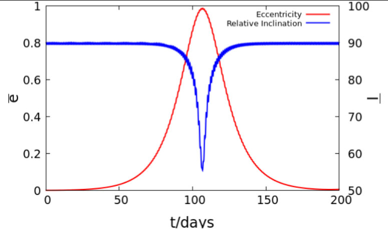

Gupta, Suzuki, Okaway and Maeda, PRD 101.104053 (2020)

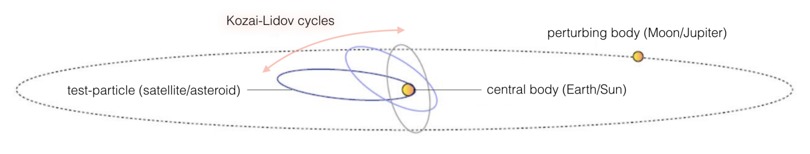

Image Credit: Konstantin Batygin

High eccentricity $\Rightarrow$ enhanced GW emission

$$\mathcal{P} \propto \frac{1}{(1-e_{\rm in}^2)^{7/2}}\left(1 + \frac{73}{24}e_{\rm in}^2 + \frac{37}{96}e_{\rm in}^4\right)$$

Numerically solve 1PN e.o.m. of triples + GWs quadrupole formula

Gupta, Suzuki, Okaway and Maeda, PRD 101.104053 (2020)

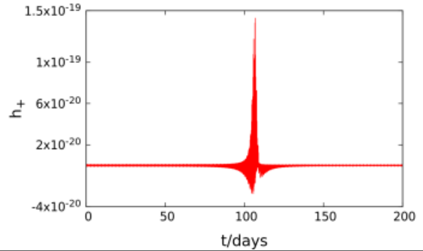

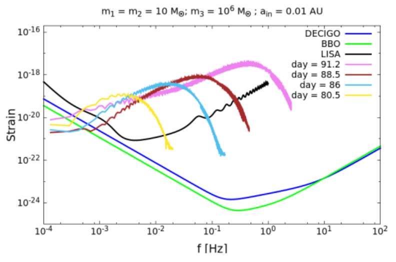

$\Uparrow \iota \Downarrow e_{in} \Rightarrow$ poor energy spectrum

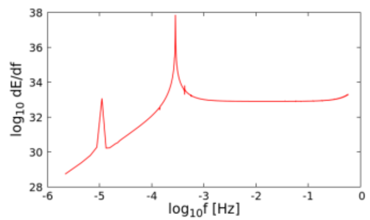

$\Downarrow \iota \Uparrow e_{in} \Rightarrow$ broad energy spectrum

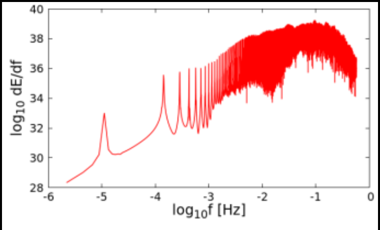

de Sitter precession: $\dot{\hat{\mathbf{L}}} = \frac{3}{2}\frac{M}{a_{\rm out}}\hat{\mathbf{L}}_{\rm out} \times \hat{\mathbf{L}}_{\rm in}$

Phenomologically model Doppler effect + de Sitter precession (1PN)

Yu and Chen, PRL 126.021101 (2021) + Randall and Xianyu, arXiv:1902.08604 (2019)

$$\tilde{h}(f) \propto exp\left\{i\left[2\Phi_T(t; M, a_{\rm out}) + \Phi_D(t; M, a_{\rm out})\right]\right\}$$

$$\Phi_T(t; M, a_{\rm out}) = -\int_0^t \left[\frac{\hat{\mathbf{L}}\times\hat{\mathbf{N}}}{1-(\hat{\mathbf{L}}\times\hat{\mathbf{N}})^2}\right]\left(\hat{\mathbf{L}}\times\hat{\mathbf{N}}\right)\dot{\hat{\mathbf{L}}}\,dt'$$

$$\Phi_D(t; M, a_{\rm out}) = -\int_0^t f(t')\,v_{\rm CM}(t')dt'$$

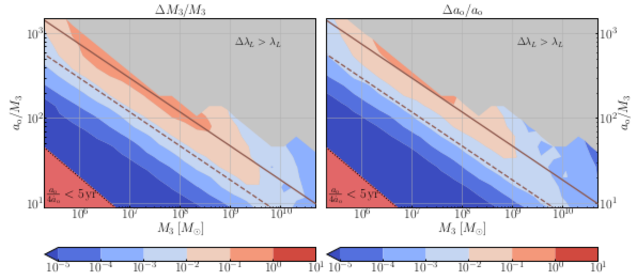

Yu and Chen, PRL 126.021101 (2021)

Gravitational Lensing

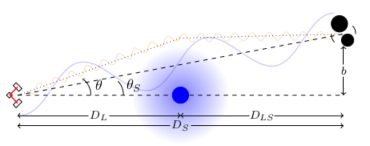

Ezquiaga, Hu and Lagos, PRD 102.023531 (2020)

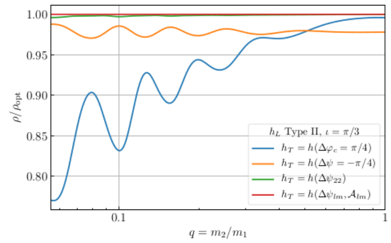

Ezquiaga, Holz, Hu, Lagos and Wald, arXiv:2008.12814 (2020)

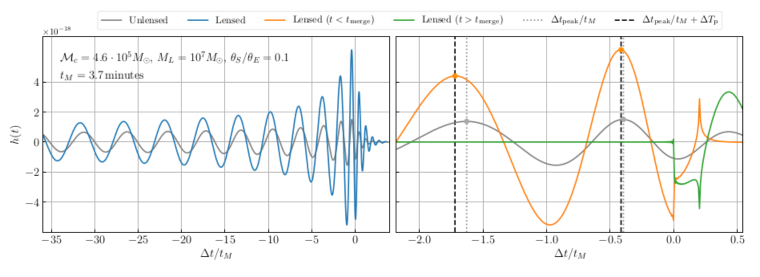

Ezquiaga, Hu and Lagos, PRD 102.023531 (2020)

Drawback

Restricted to weak field

&

Phenomelogical models

Our strategy: EMRIs *Cardoso, Duque and Khanna, arXiv:2101.01186 (2021)*

Idea: small binary perturbes background spacetime of SMBH (Kerr)

Step 1: use Teukolsky's equation *Teukolsky, ApJ 185:635-647 (1973)*

$$\mathcal{L}_s \Psi_s = \mathcal{T}_s$$

- s: spin-weight of the field ($s = \pm 2$ for GWs)
- $\mathcal{L}_s$: second-order differential operator
- Ψ_s: radiation field ($\Psi_{-2} = \ddot{h}_+ + i\ddot{h}_\times$)
- $\mathcal{T}_s$: source term describing the small binary

Step 2: Prescribe the motion of the small binary

Step 3: Solve (numerically) Teukolsky's equation
Sundarajan, Khanna and Hughes, PRD 76.104005 (2007)

Klein-Gordon equation (Teukolsky's equation when $s = 0$)

$$\Box\Psi = \alpha T$$

For point particles

$$T^{\mu\nu}(x)^{\pm} = m_0^{\pm} \frac{dt}{d\tau} \frac{dz^{\mu}}{dt} \frac{dz^{\nu}}{dt} \frac{\delta(r - r_0(t))}{r^2} \delta^{(2)}(\Omega - \Omega_0(t)) \,,$$

Frequency domain: Fourier modes + spheroidal harmonics

$$\begin{aligned} \Psi &= \sum_{\ell,m} \int \frac{d\omega}{\sqrt{2\pi}} e^{-i\omega t + im\phi} \frac{Z_{\ell m}(\omega, r)}{\sqrt{r^2 + a^2}} S_{\ell m}(\theta) \\ \Sigma T &= \sum_{\ell,m} \int \frac{d\omega}{\sqrt{2\pi}} e^{-i\omega t + im\phi} T_{\ell m}(\omega) S_{\ell m}(\theta) \end{aligned}$$

Klein-Gordon separates

$$\frac{d^2 Z_{\ell m}}{dr_*^2} + V Z_{\ell m} = \alpha \frac{\Delta}{(r^2 + a^2)^{3/2}} T_{\ell m}$$

Define two linear independent homogeneous solutions

$$
\begin{aligned}
Z_1(\omega, r) &\sim e^{-i(\omega - m\Omega_H)r_*}\,, && r_* \to -\infty \\
&\sim A_{\rm in} e^{-i\omega r_*} + A_{\rm out} e^{i\omega r_*}\,, && r_* \to +\infty \\
Z_2(\omega, r) &\sim e^{i\omega r_*}\,, && r_* \to +\infty
\end{aligned}
$$

Green's function techniques gives solution

$$
\begin{aligned}
Z_{\ell m}(r) &= \alpha \int dr' G(r, r') \frac{T_{\ell m}(r')}{(r'^2 + a^2)^{1/2}} \\
G(r, r') &= \frac{\theta(r' - r) Z_2(r') Z_1(r) + \theta(r - r') Z_2(r) Z_1(r')}{2 i \omega A_{in}}
\end{aligned}
$$

Take elliptical orbits around the CM

$$r^{\pm} = R_{\text{CM}} \quad , \quad \phi^{\pm} = \Omega_{\mathrm{CM}} t \pm \epsilon_\phi \sin \omega_0 t \quad , \quad \theta^{\pm} = \pi/2 \pm \epsilon_\theta \cos \omega_0 t$$

At $r \to \infty$

$$Z_{\ell m} = e^{i\omega r_*} \frac{\sqrt{2\pi}\, m_0}{\sqrt{R^2 + a^2}\, U^t_{\mathrm{CM}}} \frac{\alpha Z_1(\omega, R)}{2i\omega A_{\mathrm{in}}} \; (A_{\mathrm{CM}} + B_+ + B_-)$$

$$\begin{aligned}
A_{\mathrm{CM}} &= \left(\left(2 - \frac{m^2 \epsilon_\phi^2}{2}\right) S^*_{\ell m}(\pi/2) \right. \\
&\quad + \left. \frac{\epsilon_\theta^2}{2} \partial_\theta S^*_{\ell m}(\pi/2) \right) \delta(\omega - m\Omega_{\mathrm{CM}}) \\
B_{\pm} &= \Big(\frac{m^2 \epsilon_\phi^2}{4} S^*_{\ell m}(\pi/2) + \frac{\epsilon_\theta^2}{4} \partial_\theta^2 S^*_{\ell m}(\pi/2) \\
&\quad \mp \epsilon_\theta \epsilon_\phi \frac{m}{2} \partial_\theta S^*_{\ell m}(\pi/2) \Big) \delta(\omega - m\Omega_{\mathrm{CM}} \pm 2\omega_0)
\end{aligned}$$

Energy Extraction

Binary w/ frequency ω_0 placed at the ISCO of BH w/ $a/M = 0.9$

$(r^{\pm} = R\,, \quad \varphi^{\pm} = \pm\epsilon_{\varphi} \sin\omega_0 t\,, \quad \theta^{\pm} = \pi/2)$

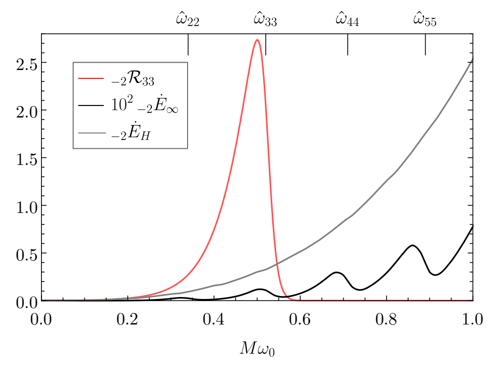

$$_s\mathcal{R}_{\ell m} = {}_s\dot{E}_{\ell m}/{}_s\dot{E}_{N\,\ell m}$$

$$_0\dot{E}_{N\,\ell m} = m_0^2\alpha^2\epsilon_{\varphi}^4 \frac{\Gamma\left(\ell + 3/2\right)}{64\sqrt{\pi}\,\ell!\,R}\, m^4\,\omega_0\, J^2_{\ell+1/2}(R\,\omega_0)$$

A detour: Purcell effect *Purcell, Phys.Rev., 69.674 (1946)*

Quantum emitter inside optical cavity

Spontaneous decay enhanced by cavity QNMs

$$\Gamma/\Gamma_0 = F\,\frac{\omega_0^2}{\omega^2}\,\frac{\omega_0^2}{\omega_0^2 + 4Q^2(\omega-\omega_0)^2}$$

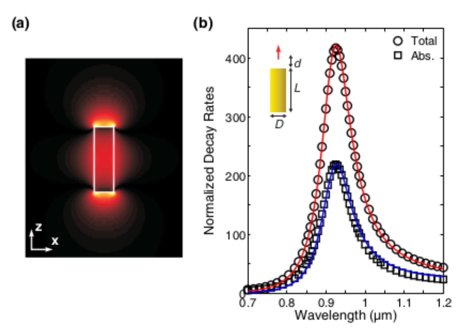

Purcell effect for metallic nanorod

Sauvan, Hugonin, Maksymov and Lalanne, PRL 110.237401 (2013)

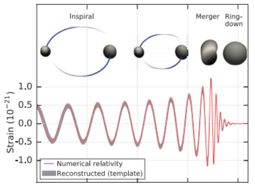

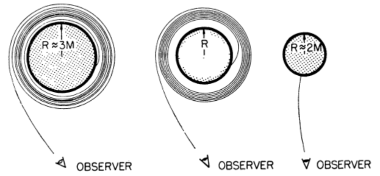

Ames and Thorne, ApJ, vol. 151, p.659 (1968)

Ringdown stage

$$h_+(t) - ih_\times(t) = \sum_{l=2}^{\infty}\sum_{m=-l}^{l}\sum_{n=0}^{\infty}\mathcal{A}_{lmn}\exp\left(i\,\omega_{lmn}t\right)_{-2}S_{lmn}$$

Non-rotating BHS have unstable null closed orbits

$$r_c = 3M \;\;,\;\; b_{\rm crit} = L_{\rm crit}/E_{\rm crit} = 3\sqrt{3}M \;\;,\;\; \Omega_{\rm LR} = 1/3\sqrt{3}M$$

Small perturbations grow exponentially

$$r = r_c + e^{\Omega_{\rm LR}\,t}$$

Eikonal limit ($l \to \infty$) *Cardoso et al., PRD, 79.064016 (2009)*

$$\omega_{lmn} = l\,\Omega_{\rm LR} - i\,(n+1/2)\,\Omega_{\rm LR}$$

Hierarchical triples behave as resonantly excited tuning forks

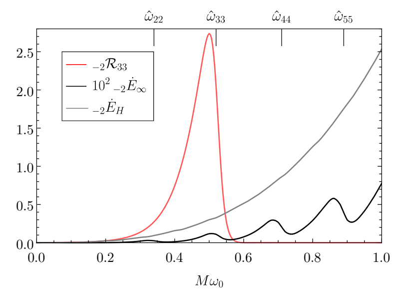

Physical principle: GW wavelength $\sim$ SMBH horizon radius

Waveforms

Binary w/ $M\omega_0 = 1$ in circular orbit at ISCO of non-spinning BH.
$(r^\pm = R\,, \quad \varphi^\pm = \Omega_{\rm CM} t \pm + \epsilon_\varphi \sin\omega_0 t\,, \quad \theta^\pm = \pi/2)$

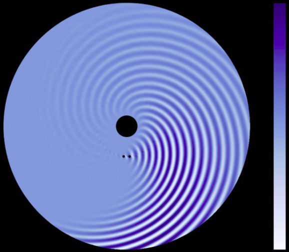

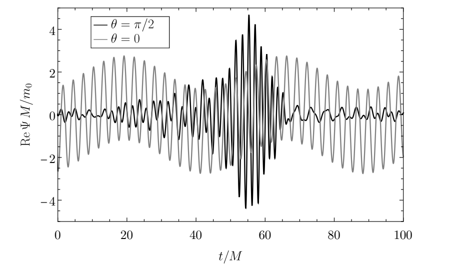

Frequency shifts: gravitational redshift + doppler effect
Cisneros, Goedecke, Beetle and Engelhardt, MNRAS 10.1093 (2015)

Amplitude modulations: gravitational lensing and relativistic beaming

Binary with $M\omega_0' = 1$ radially infalling from rest at $r = 30M$.
$(r^{\pm} = R(t)\,, \quad \varphi^{\pm} = \pm\epsilon_\varphi \sin\omega_0' t\,, \quad \theta^{\pm} = \pi/2)$

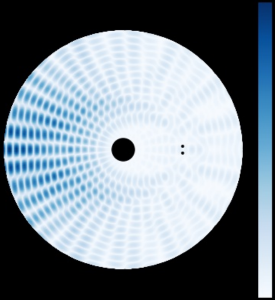

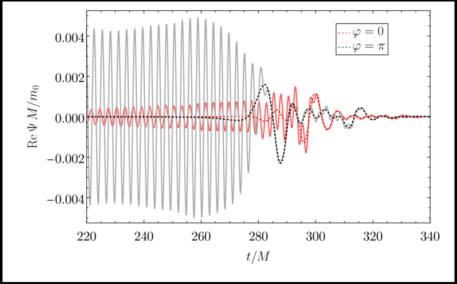

Relative motion of the binary leads to redshift/blueshift

Imprints of the binary are present in the ringdown stage

Hierarchical triple systems naturally probe strong-field gravity

Periodic Dying Flares

Flares in OJ287

Models of flares in Sgr A*

Gravity Collaboration, A&A 635, A143 (2020)

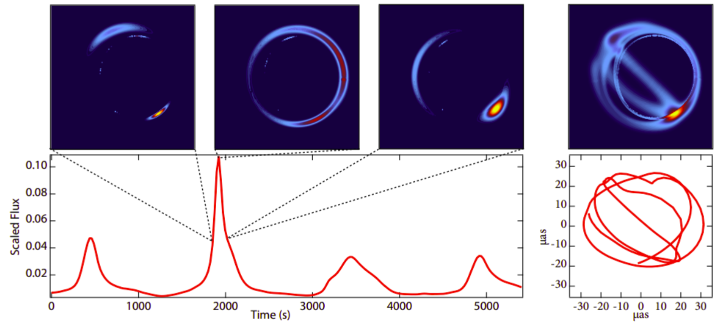

Also observed in GSN 069, Cygnus X-1...

De Luca et al., A&A 634, L13 (2020) + Dolan, PASP 113 974 (2001)

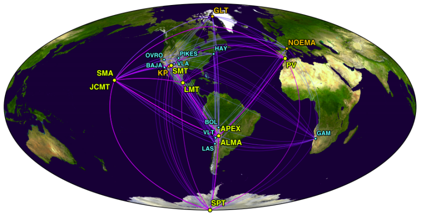

ngEHT stations

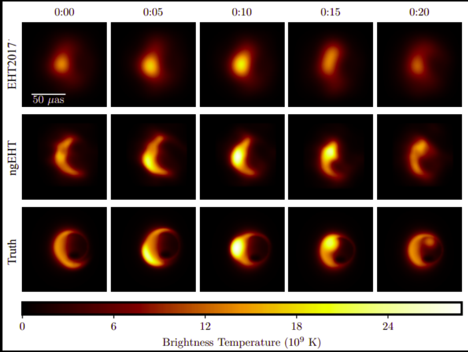

Reconstruction of flares from Sgr A*

Blackburn et al., arXiv:1909.01411 (2019)

Accretion of infalling matter *Cardoso, Duque and Foschi, arXiv:2102.07784 (2021)*

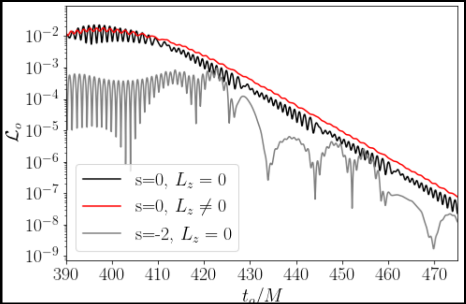

Late time behavior follows global exponential decay

$$\mathcal{L}_o \propto \exp(-\Omega_{\rm LR}\, t)$$

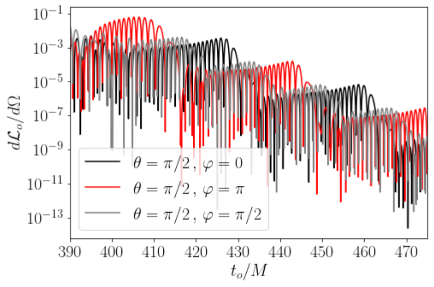

Scalar waves

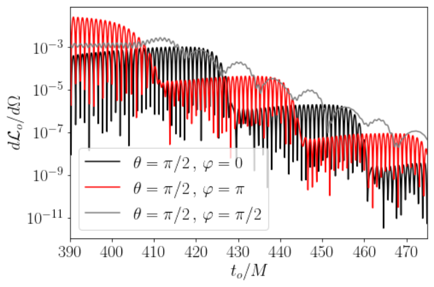

GWs

Global LR decay independent of observer's position

Spectral content dominated by blueshifted radiation $\omega_o/\omega_e \sim 1.2 - 1.3$

Periodic structures w/ frequency $n\,\Omega_{\rm LR}/2\,,\ n \in \mathbb{N}$

Geometric optics: Beam vs Isotropic star

Infalling emitter w/ proper frequency ω_e

$$\begin{aligned} v_e^\mu &= (1/f_e, -x_e, 0, 0) \quad , \quad x_e \equiv \sqrt{2M/r_e} \quad , \quad f_e \equiv 1 - 2M/r_e \\ \omega_e &= -(v_\mu k^\mu)_e \quad , \quad k^\mu\text{: photon's 4-momentum} \end{aligned}$$

Static far-away observer

$$v_o^\mu = (1, 0, 0, 0) \quad , \quad \omega_o = -(v_\mu k^\mu)_o$$

Beam: collimated pointing radially outwards

$$k^\mu = E(1/f, 1, 0, 0) \Rightarrow \omega_o = \omega_e(1 - x_e)$$

Close to the horizon

$$\begin{aligned} \frac{dr_e}{dt_e} &= -\sqrt{\frac{2M}{r_e}} f_e \Rightarrow t_e \sim -2M \log(r_e - 2M) \\ t_o &= t_e + (r_o - r_e) + 2M \log \frac{r_o - 2M}{r_e - 2M} \Rightarrow r_e - 2M \propto e^{-t_o/4M} \\ \omega_o &\sim r_e - 2M \Rightarrow \omega_o \sim e^{-t_o/4M} \Rightarrow \mathcal{L}_o \propto \omega_o^2 \sim e^{-t_o/2M} \end{aligned}$$

Star: isotropic in rest frame

$$\omega_o = \omega_e(1 + x_e \cos\alpha) \quad , \quad b = \frac{L}{E} = r_e \frac{\sin\alpha}{1 + x_e \cos\alpha}$$

α: angle ray does w.r.t. radial direction

$\alpha = \pi \Rightarrow$ Recover beam scenario

$b < b_{\rm crit} = 3\sqrt{3}M \Rightarrow$ particle falls into BH

$b = b_{\rm crit} \Rightarrow \frac{\omega_o}{\omega_e} = \frac{r_e^3 + \sqrt{2M}\sqrt{r_e^5 - b^2 r_e^2 (r_e - 2M)}}{2Mb^2 + r_e^3}$

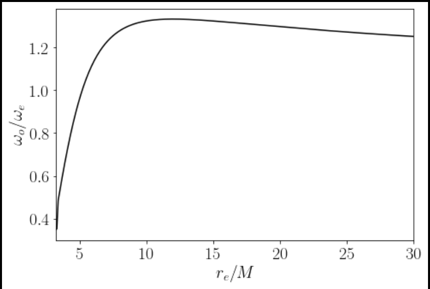

Near-critical blueshift

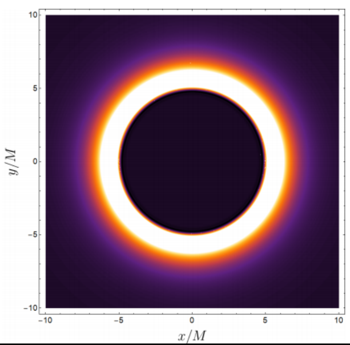

Cardoso and Vicente, PRD 100.084001 (2019)

Numerical results

All directions

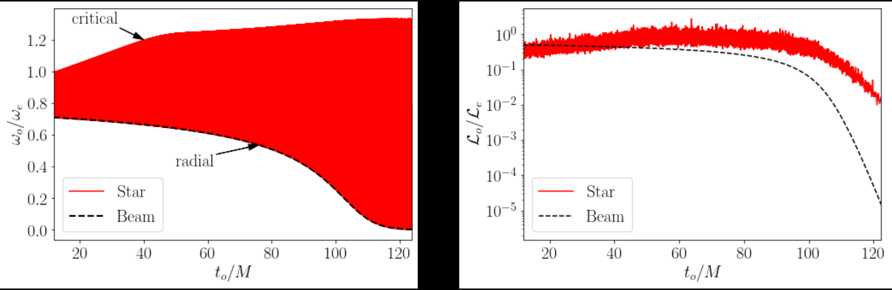

At late times

$$\left(\frac{\mathcal{L}_o}{\mathcal{L}_e}\right)_{\text{Beam}} \propto e^{-t/2M} \quad \text{vs} \quad \left(\frac{\mathcal{L}_o}{\mathcal{L}_e}\right)_{\text{Star}} \propto e^{-\Omega_{\text{LR}}\, t}$$

Testing horizons:

- Turn off the source at radius close to LR
- Increase luminosity close to LR (x10)

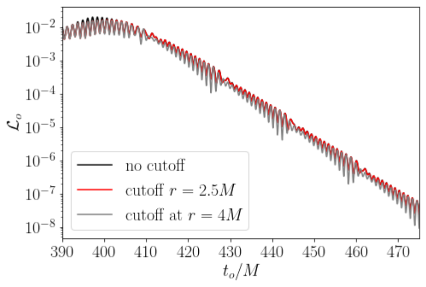

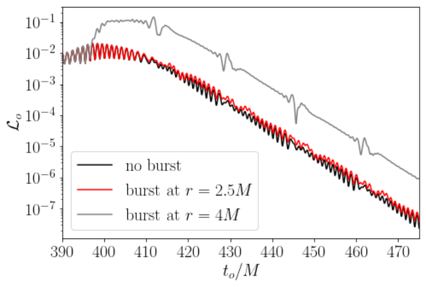

Near-horizon details not relevant for how we observe accretion

Cardoso, Franzin and Pani, PRL 116.171101 (2016)

Late time appearance of infalling matter is controlled by the light ring

Different compact objects (mass, spin, etc.)

$\Downarrow$

Different light-rings

$\Downarrow$

Different redshift/luminosity decays

$\Downarrow$

Test nature of compact objects from accreted matter's redshift/luminosity

Future Directions

Take-home message

Hierarchical triple systems naturally probe strong-field gravity

Late time appearance of infalling matter is controlled by the LR

Open problems

Detectability by GW detectors + comparison w/ weak-field

Superradiance imprints: floating orbits?
Press and Teukolsky , Nature 238 211-212 (1972)

Excitation of global properties of binary systems
Bernard, Cardoso, Ikeda and Zilhão , PRD 100.044002 (2019)

Spinning BHs: larger relaxation + break of angular degeneracies

Time-domain: two-step, second-order Lax-Wendroff finite-difference

Asymptotic behavior

$$\lim_{r\to\infty} |\Psi_s| \quad \sim \quad \begin{cases} 1/r^{2s+1} & \text{outgoing} \\ 1/r & \text{ingoing} \end{cases}$$

$$\lim_{r\to r_+} |\Psi_s| \quad \sim \quad \begin{cases} 1 & \text{outgoing} \\ \Delta^{-s} & \text{ingoing} \end{cases}$$

Evolution equations

$$\left(\partial_t + \mathbf{M}\partial_{r^*} + \mathbf{L}\right)\mathbf{u} = \mathbf{T} \;\;, \;\; \Psi\left(t, r, \theta, \varphi\right) = e^{im\tilde{\varphi}} r^{-(2s+1)} \psi\left(t, r, \theta\right)$$

where

$$\mathbf{u} \quad = \quad \left(\psi_R, \psi_I, \Pi_R, \Pi_I\right)^{\mathsf{T}}$$

$$\mathbf{M} \quad = \quad \begin{pmatrix} -b & 0 & 0 & 0 \\ 0 & -b & 0 & 0 \\ \beta^R & -\beta^I & b & 0 \\ \beta^I & \beta^R & 0 & b \end{pmatrix} \;, \; \mathbf{L} = \begin{pmatrix} 0 & 0 & -1 & 0 \\ 0 & 0 & 0 & -1 \\ \gamma^R & -\gamma^I & C_t^R & -C_t^I \\ \gamma^I & \gamma^R & C_t^I & C_t^R \end{pmatrix}$$

$$\left(\partial_t + \mathbf{D}\partial_{r^*}\right)\mathbf{u} = \mathbf{S}$$

where

$$\mathbf{D} = \mathrm{diag}\left(-b, -b, b, b\right) \ , \ \mathbf{S} = -\left(\mathbf{M} - \mathbf{D}\right)\partial_{r^*}\mathbf{u} - \mathbf{L}\,\mathbf{u} + \mathbf{T}$$

Step 1. compute solution between grid points

$$\mathbf{u}_{i+1/2}^{n+1/2} = \frac{1}{2}\left(\mathbf{u}_{i+1}^{n} + \mathbf{u}_{i}^{n}\right) - \frac{\delta t}{2}\left[\frac{1}{\delta r^*}\mathbf{D}_{i+1/2}^{n}\left(\mathbf{u}_{i+1}^{n} - \mathbf{u}_{i}^{n}\right) - \mathbf{S}_{i+1/2}^{n}\right]$$

Step 2. update solution at next time step

$$\mathbf{u}_{i}^{n+1} = \mathbf{u}_{i}^{n} - \delta t\left[\frac{1}{\delta r^*}\mathbf{D}_{i}^{n+1/2}\left(\mathbf{u}_{i+1/2}^{n+1/2} - \mathbf{u}_{i-1/2}^{n+1/2}\right) - \mathbf{S}_{i}^{n+1/2}\right]$$

Star starts at $r_e \sim 30M$ + specific observers at $r_o = 100M$

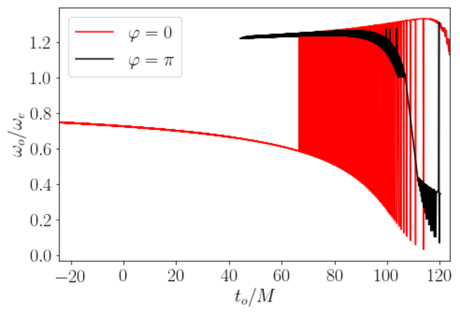

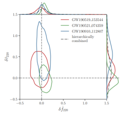

Early times:

$\varphi = 0$ radial redshifted *vs* $\varphi = \pi$ critical blueshifted after $\Delta_2 t \sim 60M$

Late times:

$\varphi = 0$ U-turn near critical blueshifted after $\Delta_1 t \sim T_{\mathrm{LR}}/2 + 60M$